JOURNAL OF AGRICULTURAL AND FOOD CHEMISTRY

Article

pubs.acs.org/JAFC

Formation of Ferric Oxyhydroxide Nanoparticles Mediated by Peptides in Anchovy (*Engraulis japonicus*) Muscle Protein Hydrolysate

Haohao Wu,[†] Zunying Liu,[†] Shiyuan Dong,[†] Yuanhui Zhao,[†] Hai Huang,[§] and Mingyong Zeng*[,†]

[†]College of Food Science and Engineering, Ocean University of China, 5 Yushan Road, Qingdao, Shandong Province 266003, China

[§]School of Aquatic Products, Rizhao Polytechnic, No. 16 North of Yantai Road, Rizhao, Shandong Province 276826, China

ABSTRACT: Nanosized iron fortificants appear to be promising and can be synthesized in a greener way using peptides as biotemplates. Anchovy is a huge underdeveloped source of muscle protein that enhances human nonheme iron absorption. This paper shows that peptides in anchovy (*Engraulis japonicus*) muscle protein hydrolysate (AMPH) mediate the formation of monodispersed ferric oxyhydroxide nanoparticles (FeONPs) with diameters of 20−40 nm above pH 3.0. Peptides in AMPH nucleate iron through carboxyl groups and crystal growth then occur as a result of condensation of carboxylate-ligated hydroxide iron centers, yielding Fe−O−Fe cross-link bonds. Monomers of FeONPs are formed after steric obstruction of further crystal growth by peptide backbones with certain lengths and further stabilized by surface-adsorbed peptides. The iron-loading capacity of peptides in AMPH is up to 27.5 mg iron/g peptide. Overall, the present study provides a greener alternative route to the synthesis of FeONPs.

KEYWORDS: *ferric oxyhydroxide, nanoparticles, peptide, anchovy, muscle protein, hydrolysate*

INTRODUCTION

Iron is an essential biological metal for many forms of life, largely due to its great variability in redox potential. Iron deficiency is a common worldwide health problem that affects more than two billion people in the world. Iron fortification of foods has been brought into practice as a cost-effective long-term approach to iron deficiency for a long time, but water solubilities of traditional iron fortificants often pose a contradiction between bioavailability and sensory quality in practice.[1] Encapsulation with edible coatings, such as polysaccharides and lipids, has been well developed to deliver soluble iron salts without reducing vehicle-food qualities,[2] and nanotechnology, which deals with materials in the nanoscale (roughly 1−100 nm), may provide another good solution to overcome this contradiction. Recent studies have found that nanonization makes poorly water-soluble iron compounds including ferric phosphate and ferric oxide/oxyhydroxide as well absorbed as freely water-soluble salts in Caco-2 cells or rats.[3−5] With less chemical reactivity than freely water-soluble iron salts, nanosized poorly water-soluble iron compounds cause fewer sensory changes in food matrices.[6] Gravitational forces at the nanoscale are weak enough to be neglected, so nanosized poorly water-soluble iron compounds are "water-soluble" and easy to deliver in aqueous food systems.[7]

Nanoparticles of poorly water-soluble iron compounds can be prepared by either a top-down or bottom-up approach. Top-down methods, such as mechanical grinding and thermal decomposition (flame spray, laser pyrolysis, plasma evaporation, etc.), require complicated instruments and much energy to reduce sizes of bulk materials to the nanoscale, so they are not convenient or energy efficient. Bottom-up approaches, such as coprecipitation, hydrothermal synthesis, and surfactant-mediated synthesis, involve controlling nucleation and crystal growth by adjusting the solution conditions (temperature, pressure, solvent, pH, ionic strength, irradiation, reducing or capping reagents, etc.).[8] Many bottom-up approaches are not suitable for production of iron fortificants due to toxicity of the residual reagents. Inspired by the biomineralization of many living organisms, peptides have been used as biotemplates to synthesize various metal nanoparticles under mild conditions in recent years, which provides a greener bottom-up approach for the production of nanosized iron fortificants.[9,10]

Fish has been considered to enhance nonheme iron absorption for a long time, and iron-binding peptides released during muscle-tissue digestion may play an important role in this enhancing effect.[11,12] Anchovy, one of the most harvested fish species worldwide today, is a cheap protein source mainly targeted for nonfood uses.[13] We previously reported enzymatic preparation and characterization of iron-binding peptides from anchovy muscle protein[14] and initially thought that iron-binding peptides would form soluble iron(III) chelates with ferric salts; however, the present study found that peptides in the anchovy muscle protein hydrolysate (AMPH) could keep an extraordinary amount of ferric iron soluble at near-neutral pH due to peptide-mediated formation of ferric oxyhydroxide nanoparticles (FeONPs). Anchovy can thus be a promising bioresource to produce nanosized iron fortificants. The present study also discussed potential mechanisms for peptide-mediated synthesis of FeONPs and iron-loading capacities of iron-binding peptides in AMPH using myosin$_{1116-1127}$ (IEELEEEIEAER, GenBank accession no. NP_002461.2) and

Received: September 15, 2012
Revised: December 12, 2012
Accepted: December 17, 2012
Published: December 17, 2012

keratin$_{14-29}$ (SGGGGGGGLGSGGSIR, GenBank accession no. NP_000217.2), two iron-binding oligopeptides previously identified from AMPH as model iron-binding peptides.

MATERIALS AND METHODS

Materials. Frozen anchovy (*Engraulis japonicus*), 5−8 cm in length, were obtained from Allen Ship Service Co. Ltd. (Shandong, China) and stored under refrigeration at −80 °C before use. Trypsin (a serine endoproteinase from bovine pancreas with a declared activity of 250 U/mg) was obtained from Sinopharm Chemical Co. Ltd. (Shanghai, China). Myosin$_{1116-1127}$, keratin$_{14-29}$, and diglutamic acid motif (Ac-EE-NH$_2$) were synthesized by ChinaPeptides Co., Ltd. (Shanghai, China) at purities >98%. The buffer compounds, 2-(*N*-morpholino)-ethanesulfonic acid (MES), piperazine-*N*,*N*′-bis(2-hydroxypropanesulfonic acid) (POPSO), and 3-(*N*-morpholino)propanesulfonic acid (MOPS), were obtained from Amresco (Solon, OH, USA). All other reagents used in this study were of analytical grade.

Preparation of AMPH. AMPH was prepared as described by Wu et al.[14] The anchovy meat, obtained after the frozen fish thawed in ice water, was homogenized in 3 volumes of water (w/v) and then hydrolyzed by trypsin with a 25:1 substrate to enzyme ratio (w/w) at 37 °C and pH 8 for 4 h with continuous magnetic stirring. After being heated in a boiling water bath for 10 min, the reaction mixture was then centrifuged at 10000*g* for 20 min. The supernatant was stored at 4 °C for no more than 48 h and filtered through 0.22 μm cellulose acetate filters before use. Peptide concentration in the supernatant was determined according to Lowry's method using bovine serum albumin (BSA) as the standard protein.[15]

Peptide-Mediated Synthesis of FeONPs. Peptide solutions were prepared by diluting AMPH or rehydrating the lyophilized synthetic peptides (myosin$_{1116-1127}$, keratin$_{14-29}$, and diglutamic acid motif) to certain concentrations using deionized water or buffered solutions. For a buffered system, freshly prepared $FeCl_3$ (1 mM) was added dropwise into the vortex-stirred peptide solution buffered with MES (30 mM) at pH 6.0, MOPS (30 mM) at pH 7.0, or POPSO (30 mM) at pH 8.0. For a nonbuffered system, the peptide solution was first acidified to pH 1.0 using 6 M hydrochloric acid and then neutralized to the desired pH upon the addition of fresh prepared $FeCl_3$ (1 mM) using 1 M sodium hydroxide. The experiments were performed at room temperature. Sample solutions were stored at 4 °C for no more than 24 h and filtered through 0.22 μm cellulose acetate filters before characterized. For solid sample analyses, samples were lyophilized and then stored in a desiccator until the start of experiments.

Characterization of FeONPs. FeONPs were characterized using ultraviolet−visible spectroscopy (UV−vis), dynamic light scattering (DLS), transmission electron microscopy (TEM), electrospray ionization−mass spectrometry (ESI-MS), circular dichroism (CD), and Fourier transform infrared spectroscopy (FT-IR). The UV−vis measurement was performed in a 1 cm cuvette using a Shimadzu UV-2550 spectrophotometer (Shimadzu, Kyoto, Japan) at room temperature. The DLS analysis was carried out on a Zetasizer Nano ZS (Malvern Instruments, Herrenberg, UK) equipped with a 633 nm He−Ne laser using a constant scattering angle of 173° at 25 ± 0.1 °C. For TEM measurements, sample solutions were dropped onto carbon-coated copper grids, allowed to air-dry, and then examined in a JEM 1200 EX (JEOL, Tokyo, Japan) electron microscope at 80 kV. For ESI-MS analysis, a sample solution (MeOH/water, 1:1) at a peptide concentration of 0.1 mM was directly flow-injected into a Micromass Q-Tof Ultima instrument (Waters, Manchester, UK) to acquire mass and collision-induced dissociation (CID) spectra in the *m*/*z* 200−2000 range, and assignment of peaks in the mass spectra was according to Loo et al.[16] Far-UV CD spectra were measured on a MOS-450 spectropolarimeter (Bio-Logic, France) using a 1 cm path length cell at room temperature. FT-IR spectra were recorded on a Nicolet iS10 FTIR spectrophotometer (Thermo Scientific, Woburn, MA, USA) using KBr pellets.

Statistical Analysis. All treatments were done in triplicate, and data are presented as the mean ± standard deviation (SD). The least significant difference (LSD) mean comparison was performed using the SPSS software program (SPSS Inc., Chicago, IL, USA) to compare the mean differences between the measurements at P = 5%.

RESULTS AND DISCUSSION

Observation of the Formation of FeONPs. After hydrolysis of the 0.1 mM $FeCl_3$ in a 30 mM MES buffer (pH 6.0), colloidal ferric oxyhydroxide was formed and showed a characteristic broad absorption band of iron oxides in the region between 250 and 500 nm (Figure 1a).[17] The absorption

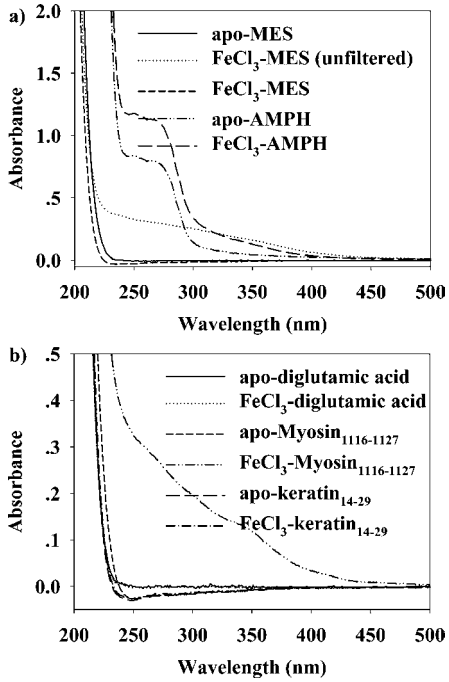

Figure 1. UV−vis spectra of apo and iron-loaded forms of (a) AMPH (0.61 g/L) and (b) diglutamic acid motif (0.1 mM), myosin$_{1116-1127}$ (0.1 mM), and keratin$_{14-29}$ (0.1 mM) in the 30 mM MES buffer at pH 6.0 with a $FeCl_3$-loading concentration of 0.1 mM. Solutions were filtered through 0.22 μm cellulose acetate filters before measurement if not mentioned.

band disappeared after the colloidal solution was filtered through 0.22 μm filters, indicating that ferric oxyhydroxide formed in the MES buffer was in fact a macroscopic precipitate. When AMPH was present in the MES buffer, 0.22 μm filtration could not reduce the absorption of already-formed ferric oxyhydroxide, suggesting the peptide-mediated formation of FeONPs. AMPH was in fact a peptide mixture, which posed a problem in gaining information about what roles peptides played in the formation of FeONPs. In this study, we synthesized two iron-binding oligopeptides previously identified from AMPH as model peptides. As shown in Figure 1b, myosin$_{1116-1127}$ with clusters of glutamic acid residues in the sequence was found to mediate the synthesis of FeONPs, whereas keratin$_{14-29}$ with several serine residues in the sequence could not. Carboxyl groups are the main iron nucleation sites for ferritin, the major iron storage protein in living organisms, and Mms6, a bacterial biomineralization protein.[18,19] According to the hard−soft-acid−base principle, alcoholic hydroxyl groups are much weaker ferric binding ligands than carboxylates and hydroxide ions.[20] Thus, serine hydroxyl groups cannot compete with hydroxide ions to bind ferric iron in aqueous solutions, which may explain the

dx.doi.org/10.1021/jf3039692 | J. Agric. Food Chem. 2013, 61, 219−224

ineffectiveness of keratin$_{14-29}$ to mediate the formation of FeONPs in this study. A diglutamic acid motif was also synthesized to illustrate whether a simple structure unit in peptides with two acidic residues can function to mediate the formation of FeONPs in this study. No FeONPs were formed in the presence of diglutamic acid motif (Figure 1b), suggesting that not only carboxyl groups but also certain lengths are required for peptides to mediate the formation of FeONPs. Carboxyl groups only provide iron nucleation sites for peptides, but peptide backbones with certain lengths could provide steric barriers to prevent further crystal growth.[21]

To determine the hydrodynamic size of FeONPs formed in a peptide solution, DLS was performed. Figure 2 shows the number size distributions of FeONPs synthesized in the presence of AMPH and myosin$_{1116-1127}$. A single maximum peak at 25 nm was observed for AMPH, whereas two maximum peaks at 15 and 41 nm could be distinguished for myosin$_{1116-1127}$. As shown in Figure 3, these nanoparticles were visualized by TEM. In case of FeONPs formed in the presence of AMPH, nearly spherical monomers with diameters in the range of 20−40 nm could be distinguished from the edge of the agglomerate, which was difficult to avoid during drying in the sample preparation. FeONPs formed in the presence of myosin$_{1116-1127}$ appeared mainly as nanoscale aggregates in the TEM image, and monomers could be vaguely distinguished with diameters of about 8−20 nm. FeONPs synthesized in the presence of AMPH seemed to be monodispersed in the solution according to their single-peak hydrodynamic size distribution, whereas monomers of FeONPs formed in the presence of myosin$_{1116-1127}$ seemed to readily aggregate into larger nanoscale polymers in light of the corresponding peaks of monomers and polymers in the double-peak hydrodynamic size distribution. Thus, FeONPs synthesized in the presence of AMPH seemed to be better stabilized than those formed in the presence of myosin$_{1116-1127}$. AMPH was in fact a cocktail of various peptides, some of which might adhere to surfaces of monomers of FeONPs through the C-terminal or side-chain carboxyl groups and stabilize them effectively. Myosin$_{1116-1127}$, a purified peptide, could mediate the formation of monomers of FeONPs, but these monomers seemed not stable enough to be completely free from aggregation unless additional capping agents had been added.[22]

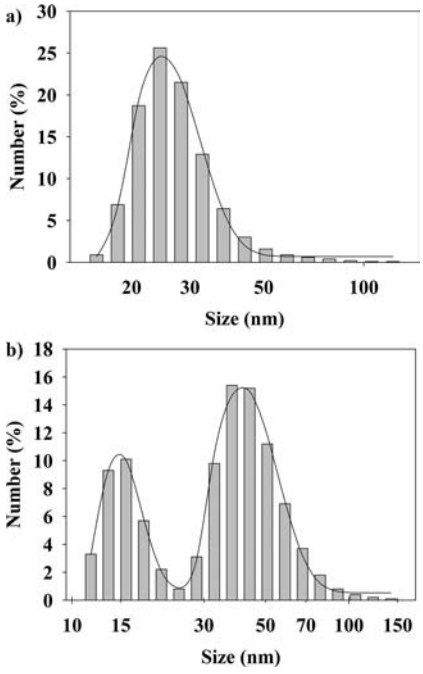

Figure 2. Size distributions of FeONPs synthesized in the presence of (a) AMPH (3.05 g/L) and (b) myosin$_{1116-1127}$ (0.1 mM) in a 30 mM MES buffer at pH 6.0 with a $FeCl_3$-loading concentration of 0.3 mM.

Potential Mechanisms for Peptide-Mediated Formation of FeONPs. Myosin$_{1116-1127}$ was used as our example to illustrate potential mechanisms for peptide-mediated formation of FeONPs. Figure 4a shows UV−vis spectra of apo and iron-loaded forms of myosin$_{1116-1127}$ at various pH levels. The absorption changed most around position 1 (250 nm) and position 2 (310 nm) at pH levels below 1.5 and between 1.5 and 3.0, respectively. The absorption band around 250 nm can be assigned to ligand to metal charge transfer (LMCT) transitions, whereas absorbance increments around 310 nm can be attributed to pair excitations of adjacent Fe^{3+} centers coupled by Fe−O−Fe superexchange.[17] The ill-defined broad absorption band of iron-loaded myosin$_{1116-1127}$ at pH 1.0 bore great resemblance to that of iron−citrate complexes at the same pH.[23] Studies on iron−citrate complexes reveal that carboxyl groups can bind iron at pH levels as low as 0.5, so myosin$_{1116-1127}$ seemed to have nucleated iron through carboxyl

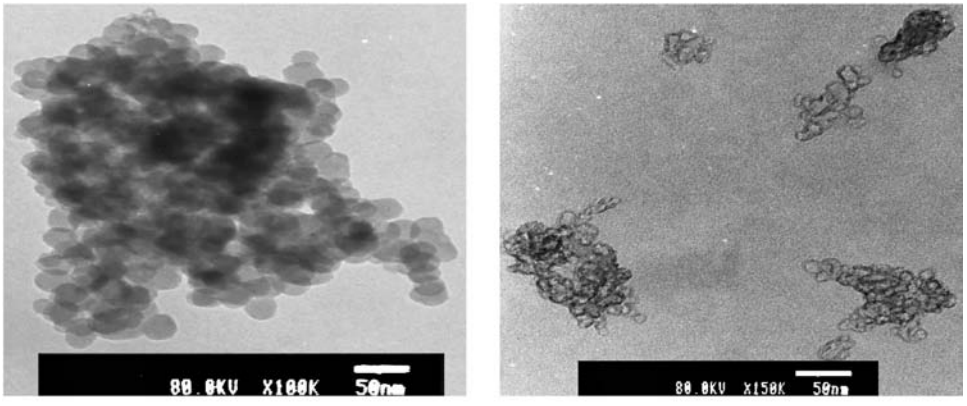

Figure 3. TEM images of FeONPs synthesized in the presence of (a) AMPH (3.05 g/L) and (b) myosin$_{1116-1127}$ (0.1 mM) in a 30 mM MES buffer at pH 6.0 with a $FeCl_3$-loading concentration of 0.3 mM.

dx.doi.org/10.1021/jf3039692 | J. Agric. Food Chem. 2013, 61, 219−224

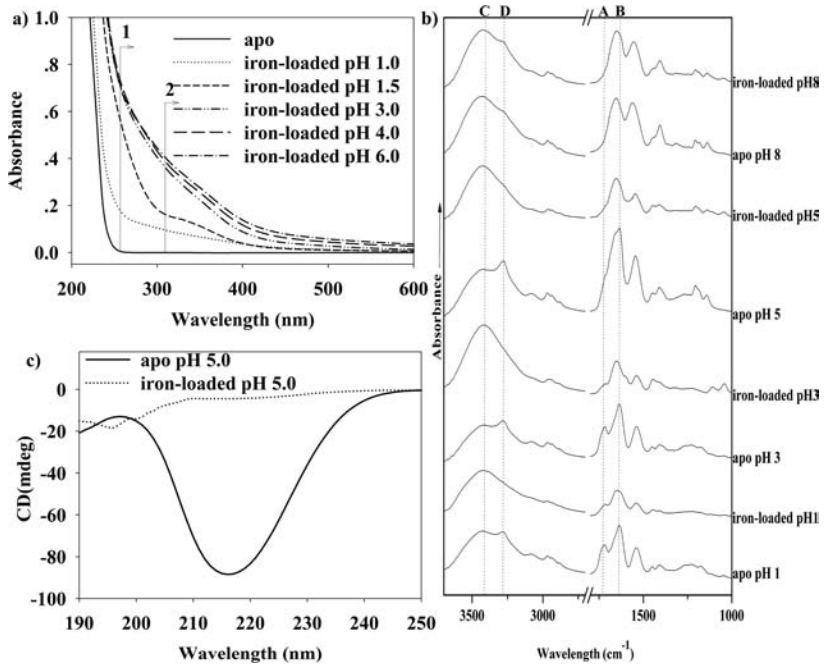

Figure 4. Characterization of apo and iron-loaded forms of myosin$_{1116-1127}$ (0.1 mM) at various pH values with a $FeCl_3$-loading concentration of 0.3 mM by (a) UV−vis, (b) FT-IR, and (c) CD. No buffer was used.

groups at pH 1.0. When the pH was elevated from 1.0 to 1.5, hydroxide ions, which ligate iron above pH 1.0, then entered the vacant orbitals of carboxylate-ligated iron to form peptide-templated hydroxide iron complexes as indicated by the increased LMCT absorption around position 1.[24] The absorption band of Fe^{3+}−Fe^{3+} pair excitations around position 2 increased dramatically in intensity in the pH range of 1.5−3.0, suggesting that crystal growth occurred as a result of condensation of carboxylate-ligated hydroxide iron centers yielding Fe−O−Fe bonds.[25] The absorption changed to a very little extent above pH 3.0, indicating that FeONPs were formed at pH levels above 3.0.

As shown in Figure 4b, FT-IR spectra for apo and iron-loaded forms of myosin$_{1116-1127}$ were recorded at various pH values. No apparent differences could be distinguished from the infrared spectra of apo and iron-loaded forms of myosin$_{1116-1127}$ at pH 8.0, which indicated that myosin$_{1116-1127}$ did not mediate the formation of FeONPs at a pH level of 8.0. Iron-loaded forms of myosin$_{1116-1127}$ at pH 1.0, 3.0, and 5.0 gave lower peak intensities at position A (1716 cm^{-1}) and increased peak intensities at position C (3420 cm^{-1}) compared with their corresponding apo forms. The absorption band at 1716 cm^{-1} can be assigned to carboxyl groups of myosin$_{1116-1127}$, and carboxyl deprotonation will lower the intensity of this IR band.[26] It thus seemed that carboxyl groups of myosin$_{1116-1127}$ deprotonated to form COO−Fe bonds at pH levels as low as 1.0, which confirmed the above-mentioned iron nucleation of myosin$_{1116-1127}$. The absorption increments at 3420 cm^{-1} can be attributed to H−O−H stretching vibration of water molecules adsorbed by under-coordinated iron atoms in iron-loaded myosin$_{1116-1127}$.[27] Unless under ultrahigh vacuum conditions, metal salts and oxides can easily adsorb H_2O on their surfaces to satisfy under-coordinated metal atoms. The huge infrared absorptions of surface-adsorbed water molecules in iron-loaded samples at pH 1.0, 3.0, and 5.0 overlapped the amide A (N−H stretch) bands of myosin$_{1116-1127}$ around position D (3280 cm^{-1}). The amide I bands of apo samples at position B (1635 cm^{-1}) were red-shifted to 1648 cm^{-1} by iron loading at pH 1.0, 3.0, and 5.0. The amide I bands at 1635 and 1648 cm^{-1} can be assigned to β-sheet and random coil structures, respectively.[28] The hydrogen bonds of myosin$_{1116-1127}$ seemed to be disrupted by iron loading, so that the β-sheet transformed into a less ordered random coil structure. As shown in Figure 4c, CD was performed to validate the secondary structural change of myosin$_{1116-1127}$ before and after iron loading at pH 5.0. The apo myosin$_{1116-1127}$ showed characteristic positive and negative CD peaks for β-sheet at 198 and 218 nm, whereas the iron-loaded myosin$_{1116-1127}$ gave a characteristic negative CD peak for random coil around 200 nm.[29] These CD results thus seemed to agree well with the results obtained by FT-IR.

Iron-Loading Capacity Studies. The amount of FeONPs formed in a peptide solution can be relatively quantified by the absorbance (OD) at 310 nm where oxo-bridged diferric centers (Fe−O−Fe) in FeONPs have a characteristic absorption band as mentioned above. The relative amount of FeONPs formed in a peptide solution generally increased linearly with the dose increment of ferric ions within a certain dose range and then decreased (Figure 5a,b). Excess ferric ions added into a peptide solution seemed to form amorphous ferric oxyhydroxide, which could adsorb and coprecipitate the already-formed FeONPs. Iron-loading capacities of peptides can thus be inferred from the dose-dependent formation of FeONPs. Both AMPH and myosin$_{1116-1127}$ have higher iron-loading capacities at pH 7.0 than at pH 6.0 and 8.0. Higher pH levels in a weakly acid environment seemed to favor peptide-mediated formation of FeONPs, possibly because iron-binding abilities of donor groups in peptides were enhanced with increasing pH levels.[30] A pH value of >7.0 lowered iron-loading capacities of peptides possibly due to the competitive binding of higher concentrations of hydroxide ions in alkaline solutions to ferric iron. Myosin$_{1116-1127}$, each molecule of which could load up to five iron atoms, had a calculated iron-loading capacity of 188.1 mg iron/g peptide at pH 7.0, whereas the iron-loading capacity of

dx.doi.org/10.1021/jf3039692 | J. Agric. Food Chem. 2013, 61, 219−224

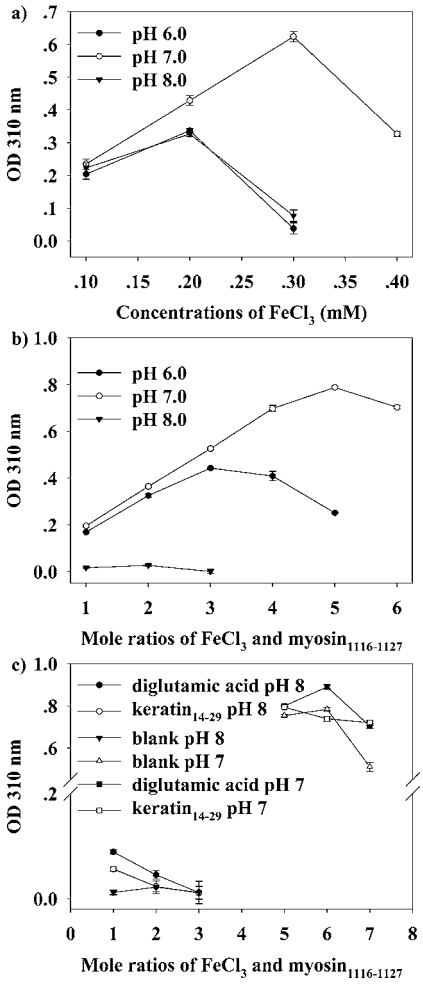

Figure 5. Amounts of FeONPs synthesized in the presence of (a) AMPH (0.61 g/L), (b) myosin$_{1116-1127}$ (0.083 mM), and (c) cocktails of myosin$_{1116-1127}$ (0.083 mM) and diglutamic acid motif or keratin$_{14-29}$ at a 1:1 molar mixing ratio as measured by OD 310 nm. Sample solutions were buffered with MES (30 mM) at pH 6.0, MOPS (30 mM) at pH 7.0, or POPSO (30 mM) at pH 8.0.

AMPH at pH 7.0 was calculated as 27.5 mg iron/g peptide. As shown in Figure 5c, diglutamic acid motif and keratin$_{14-29}$, neither of which could mediate the formation of FeONPs on their own as mentioned above, enhanced the iron-loading capacity of myosin$_{1116-1127}$ at pH 7.0. Myosin$_{1116-1127}$ in fact did not mediate the formation of any FeONPs on its own at pH 8.0 (Figure 5b), but some FeONPs were formed when myosin$_{1116-1127}$ coexisted with diglutamic acid motif or keratin$_{14-29}$ at pH 8.0 (Figure 5c). Thus, peptides that are unable to mediate the formation of FeONPs on their own seem to provide synergy for other peptides in the synthesis of FeONPs.

ESI-MS was performed to visualize molecules of iron-loaded myosin$_{1116-1127}$ (Figure 6a). Up to four ferric ions bound to each molecule of myosin$_{1116-1127}$ as demonstrated by the peaks at m/z 833.5, 851.5, 868.5, and 886.5, which were assigned to $[M + 3Fe^{3+} + O^{2-} - 5H^+]^{2+}$, $[M + 3Fe^{3+} + O^{2-} + 2OH^- - 3H^+]^{2+}$, $[M + 4Fe^{3+} + 2O^{2-} - 6H^+]^{2+}$, and $[M + 4Fe^{3+} + 2O^{2-} + 2OH^-]^{2+}$, respectively. These binding patterns agreed well with the above-mentioned formation of COO−Fe, Fe−O−Fe, and Fe−OH bonds in the peptide-mediated synthesis of FeONPs. ESI-MS/MS of the parent ion of m/z 868.5 was performed to confirm multiple ferric ions bound to myosin$_{1116-1127}$. As shown in Figure 6b, the parent ion of m/z 868.5 fragmented into ions at m/z 781.5, 790.0, 833.6, and 851.6, which could be assigned to $[M + Fe^{3+} + OH^-]^{2+}$, $[M + Fe^{3+} + 2OH^- + H^+]^{2+}$, $[M + 3Fe^{3+} + O^{2-} - 5H^+]^{2+}$, and $[M + 3Fe^{3+} + O^{2-} + 2OH^- - 3H^+]^{2+}$, respectively. One or three ferric ions in $[M + 4Fe^{3+} + 2O^{2-} - 6H^+]^{2+}$ thus seemed to be knocked out by CID.

Overall, the present study provides a greener alternative route to the synthesis of FeONPs. Further studies are needed to explore potential applications of peptides originated from food proteins in the production of nanosized iron fortificants.

AUTHOR INFORMATION

Corresponding Author

*Fax: +86 0532 82032400. E-mail: mingyz@ouc.edu.cn.

Funding

This work was financially supported by the National Natural Science Foundation of China (No. 31101379).

Notes

The authors declare no competing financial interest.

ABBREVIATIONS USED

FeONPs, ferric oxyhydroxide nanoparticles; AMPH, anchovy muscle protein hydrolysate; MES, 2-(*N*-morpholino)-ethanesulfonic acid; POPSO, piperazine-*N*,*N*′-bis(2-hydroxy-

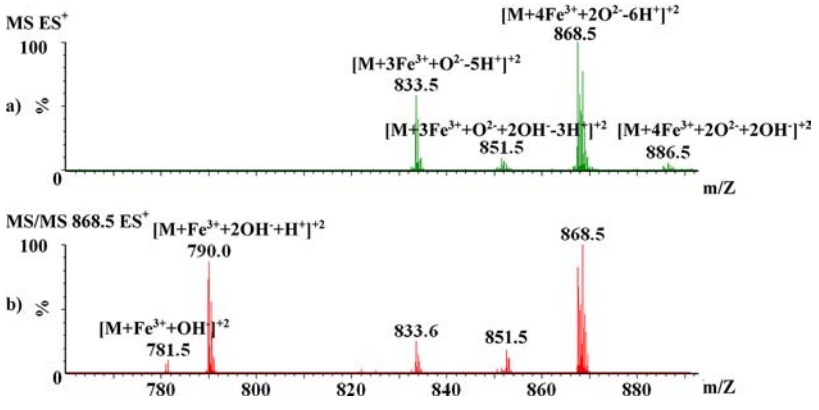

Figure 6. (a) ESI-MS spectra of FeONPs synthesized in the presence of myosin$_{1116-1127}$ (0.1 mM) at pH 7.0 with a $FeCl_3$-loading concentration of 0.5 mM; (b) MS/MS spectra for the parent ion of m/z 868.5. No buffer was used. M represents the mass of myosin$_{1116-1127}$.

dx.doi.org/10.1021/jf3039692 | *J. Agric. Food Chem.* 2013, 61, 219−224

propanesulfonic acid); MOPS, 3-(*N*-morpholino)-propanesulfonic acid; CID, collision-induced dissociation; LMCT, ligand to metal charge transfer

REFERENCES

(1) WHO/UNICEF/UNU. *Iron Deficiency Anemia Assessment, Prevention, and Control*; World Health Organization: Geneva, Switzerland, 2001.

(2) Zimmermann, M. B.; Windhab, E. J. Encapsulation of iron and other micronutrients for food fortification. In *Encapsulation Technologies for Active Food Ingredients and Food Processing*; Zuidam, N. J., Nedovic, V. A., Eds.; Springer-Verlag: New York, 2010; pp 187−210.

(3) Rohner, F.; Ernst, F. O.; Arnold, M.; Hilbe, M.; Biebinger, R.; Ehrensperger, F.; Pratsinis, S. E.; Langhans, W.; Hurrell, R. F.; Zimmermann, M. B. Synthesis, characterization, and bioavailability in rats of ferric phosphate nanoparticles. *J. Nutr.* **2007**, *137*, 614−619.

(4) Hilty, F. M.; Arnold, M.; Hilbe, M.; Teleki, A.; Knijnenburg, J. T.; Ehrensperger, F.; Hurrell, R. F.; Pratsinis, S. E.; Langhans, W.; Zimmermann, M. B. Iron from nanocompounds containing iron and zinc is highly bioavailable in rats without tissue accumulation. *Nat. Nanotechnol.* **2010**, *5*, 374−380.

(5) Jahn, M. R; Nawroth, T.; Fütterer, S.; Wolfrum, U.; Kolb, U.; Langguth, P. Iron oxide/hydroxide nanoparticles with negatively charged shells show increased uptake in Caco-2 cells. *Mol. Pharmaceutics* **2012**, *9*, 1628−1637.

(6) Hilty, F. M.; Knijnenburg, J. T.; Teleki, A.; Krumeich, F.; Hurrell, R. F.; Pratsinis, S. E.; Zimmermann, M. B. Incorporation of Mg and Ca into nanostructured Fe_2O_3 improves Fe solubility in dilute acid and sensory characteristics in foods. *J. Food Sci.* **2011**, *76*, N2−N10.

(7) Roduner, E. Size matters: why nanomaterials are different. *Chem. Soc. Rev.* **2006**, *35*, 583−592.

(8) Mohapatra, M.; Anand, S. Synthesis and applications of nano-structured iron oxides/hydroxides − a review. *Int. J. Eng. Sci. Technol.* **2010**, *2*, 127−146.

(9) Galloway, J. M.; Staniland, S. S. Protein and peptide biotemplated metal and metal oxide nanoparticles and their patterning onto surfaces. *J. Mater. Chem.* **2012**, *22*, 12423−12434.

(10) Tan, Y. N.; Lee, J. Y.; Wang, D. I. Uncovering the design rules for peptide synthesis of metal nanoparticles. *J. Am. Chem. Soc.* **2010**, *132*, 5677−5686.

(11) Cook, J. D.; Monsen, E. R. Food iron absorption in human subjects. III. Comparison of the effects of animal proteins on nonheme iron absorption. *Am. J. Clin. Nutr.* **1976**, *29*, 859−867.

(12) Storcksdieck, S.; Bonsmann, G.; Hurrell, R. F. Iron-binding properties, amino acid composition, and structure of muscle tissue peptides from in vitro digestion of different meat sources. *J. Food Sci.* **2007**, *72*, S019−S029.

(13) Food and Agriculture Organization of the United Nations. Global Capture Production 1950−2010; http://www.fao.org/fishery/statistics/global-capture-production/query/en (accessed Sept 2012).

(14) Wu, H.; Liu, Z.; Zhao, Y.; Zeng, M. Enzymatic preparation and characterization of iron-chelating peptides from anchovy (*Engraulis japonicus*) muscle protein. *Food Res. Int.* **2012**, *48*, 435−441.

(15) Lowry, O. H.; Rosebrough, N. J.; Farr, A. L.; Randall, R. J. Protein measurement with the Folin phenol reagent. *J. Biol. Chem.* **1951**, *193*, 265−275.

(16) Loo, J. A.; Hu, P.; Smith, R. D. Interaction of angiotensin peptides and zinc metal ions probed by electrospray ionization mass spectrometry. *J. Am. Soc. Mass Spectrom.* **1994**, *5*, 959−965.

(17) Sherman, D. M.; Waite, T. D. Electronic spectra of Fe^{3+} oxides and oxide hydroxides in the near IR to near UV. *Am. Mineral.* **1985**, *70*, 1262−1269.

(18) Granier, T.; Langlois d'Estaintot, B.; Gallois, B.; Chevalier, J. M.; Précigoux, G.; Santambrogio, P.; Arosio, P. Structural description of the active sites of mouse L-chain ferritin at 1.2 A resolution. *J. Biol. Inorg. Chem.* **2003**, *8*, 105−111.

(19) Wang, L.; Prozorov, T.; Palo, P. E.; Liu, X.; Vaknin, D.; Prozorov, R.; Mallapragada, S.; Nilsen-Hamilton, M. Self-assembly and biphasic iron-binding characteristics of Mms6, a bacterial protein that promotes the formation of superparamagnetic magnetite nanoparticles of uniform size and shape. *Biomacromolecules* **2012**, *13*, 98−105.

(20) Carey, F. A.; Sundberg, R. J. *Advanced Organic Chemistry: Part A: Structure and Mechanisms*, 5th ed.; Springer: Berlin, Germany, 2007; pp 407−409.

(21) Gerbaud, V.; Pignol, D.; Loret, E.; Bertrand, J. A.; Berland, Y.; Fontecilla-Camps, J. C.; Canselier, J. P.; Gabas, N.; Verdier, J. M. Mechanism of calcite crystal growth inhibition by the N-terminal undecapeptide of lithostathine. *J. Biol. Chem.* **2000**, *275*, 1057−1064.

(22) Iijima, M.; Kamiya, H. Surface modification for improving the stability of nanoparticles in liquid media. *KONA* **2009**, *27*, 119−129.

(23) Vukosav, P.; Mlakar, M.; Tomišić, V. Revision of iron(III)-citrate speciation in aqueous solution. Voltammetric and spectrophotometric studies. *Anal. Chim. Acta* **2012**, *745C*, 85−91.

(24) Stefánsson, A. Iron(III) hydrolysis and solubility at 25 °C. *Environ. Sci. Technol.* **2007**, *41*, 6117−6123.

(25) Stumm, W.; Morgan, J. J. *Aquatic Chemistry, Chemical Equilibria and Rates in Natural Waters*, 3rd ed.; Wiley: New York, 1996; pp 263−264.

(26) Barth, A.; Zscherp, C. What vibrations tell us about proteins. *Q. Rev. Biophys.* **2002**, *35*, 369−430.

(27) Kubicki, J. D.; Paul, K. W.; Sparks, D. L. Periodic density functional theory calculations of bulk and the (010) surface of goethite. *Geochem. Trans.* **2008**, *9*, 4.

(28) Kong, J.; Yu, S. Fourier transform infrared spectroscopic analysis of protein secondary structures. *Acta Biochim. Biophys. Sin. (Shanghai)* **2007**, *39*, 549−559.

(29) Corrêa1, D. H. A.; Ramos, C. H. I. The use of circular dichroism spectroscopy to study protein folding, form and function. *Afr. J. Biochem. Res.* **2009**, *3*, 164−173.

(30) Kállay, C.; Várnagy, K.; Micera, G.; Sanna, D.; Sóvágo, I. Copper(II) complexes of oligopeptides containing aspartyl and glutamyl residues. Potentiometric and spectroscopic studies. *J. Inorg. Biochem.* **2005**, *99*, 1514−1525.